Chin. Sci. Bull. (2014) 59(20):2460–2469
DOI 10.1007/s11434-014-0235-4 csb.scichina.com

Article Engineering Thermophysics

Self-heating dependent characteristic of GaN-based light-emitting diodes with and without AlGaInN electron blocking layer

Tianhu Wang · Jinliang Xu · Xiaodong Wang

Received: 7 April 2013 / Accepted: 24 July 2013 / Published online: 19 March 2014

Abstract In this study, GaN-based light-emitting diodes (LEDs) with and without AlGaInN electron blocking layer (EBL) under self-heating effect are numerically studied. The energy band diagram, carrier transport and distribution characteristics, internal Joule heat and non-radiative recombination heat characteristics, and internal quantum efficiency are investigated. The effect of Auger recombination coefficient on efficiency droop under self-heating effect is also studied. The simulation results show that efficiency droop is markedly improved when an AlGaInN EBL is placed between p-type GaN layer and active region. However, the chip temperature of LED is significantly increased simultaneously. The results also indicate that Auger recombination can be neglected because it is not the major contributor for the internal heat source. The efficiency droop is unrelated to the internal heat source. However, both electron leakage and Auger recombination play important roles in efficiency droop mechanism under self-heating effect.

Keywords Light-emitting diodes · Efficiency droop · Self-heating · Electron blocking layer · Auger recombination

T. Wang
Beijing Key Laboratory of New and Renewable Energy, North China Electric Power University, Beijing 102206, China

J. Xu (✉) · X. Wang (✉)
Beijing Key Laboratory of Multiphase Flow and Heat Transfer for Low Grade Energy, North China Electric Power University, Beijing 102206, China
e-mail: xjl@ncepu.edu.cn

X. Wang
e-mail: wangxd99@gmail.com

1 Introduction

The organic and nitride-based LEDs have been received great attention due to their prospective applications in medical diagnostics, optical storage, full color display, and solid state lighting [1–10]. However, when injection current is larger than typically a few milliamperes, the internal quantum efficiency of the devices suffers from a rapid reduction with increasing injection current [11–13]. This phenomenon, called efficiency droop, is a serious restriction for high brightness and high power applications of LEDs. Various techniques and designs have been proposed to improve the efficiency droop, such as optimizing the structure of quantum wells [5, 14–19], quantum barriers [20–26], electron blocking layer [13, 27–32], and last barrier [33–37] as well as reducing the internal polarization effect [11, 12, 15, 20, 21]. Among these investigations, several possible physical mechanisms leading to efficiency droop have been proposed, including current leakage from the active region [11–13, 30, 34, 35], quantum confined Stark effect in the active region [15, 18], insufficient hole injection efficiency [25, 26, 31, 32], Auger recombination [38, 39], self-heating effect, etc. [40, 41]. However, these explanations are still controversial, and the efficiency droop has not been well understood at this stage.

In the studies of EBL structure optimization to improve the efficiency droop, many reports indicate that a p-type AlGaN layer inserted between the p-type GaN layer and active region can prevent the electron overflow effectively, the LED with a p-type EBL has better performance than the LED without an EBL [27, 29, 42]. However, Ryu et al. [43] reported that the LED without an EBL structure is advantageous for achieving high internal quantum efficiency than that of the LED with an EBL. Yen et al. [28] proposed an n-type AlGaN EBL below the active region to replace the

SCIENCE CHINA PRESS

traditional p-type AlGaN EBL, the efficiency droop is improved when the p-type AlGaN EBL was removed. It is mainly due to the sufficiently reduced electron leakage and more uniform distribution of holes in the quantum wells. The effect of EBL on the efficiency droop in InGaN/GaN LEDs is systematically investigated by Han et al. [27], they reported that the efficiency droop in the LED without an EBL was suppressed at high current density due to the increased hole injection efficiency. Thus, there exists a debate on whether introducing an EBL. Furthermore, isothermal models were adopted in these studies [27, 28, 30, 31], so that the self-heating effect was neglected. Therefore, it is worthy to investigate the effect of EBL on the LED performance under self-heating effect to reveal some mechanisms.

Some studies confirmed that the internal heat has strong effect on the LED performance and efficiency droop. Chen et al. [41] reported that heat generated inside the LED can reduce both the internal and external quantum efficiencies especially at large injected current. Efremov et al. [40] studied effects of temperature, injection current as well as size and material of the heat sink on the light output and efficiency of blue LEDs. It is shown that under high injection current, the decrease in efficiency of the LED is caused by Joule heating and the temperature significantly influences the efficiency of carrier injection into the QW. Wang et al. [14] investigated the temperature-dependent electroluminescence efficiency for blue InGaN/GaN LEDs with different well widths. They found that the injection current to reach the maximum electroluminescence efficiency is strongly dependent on the well widths and temperatures. On the contrary, Kim et al. [11] reported experimentally that the magnitude of droop decreases with increasing temperature, and thus, temperature does not cause efficiency droop. In Crawford's work [3], it is indicated that the efficiency droop is not caused by simple heating, but occurs under both self-heating and non self-heating conditions. Therefore, a consensus on the mechanism behind the efficiency droop with self-heating effect remains unclear.

In this paper, two LEDs with and without an AlGaInN EBL under self-heating effect are investigated to clarify the effect of EBL on the LED performance when taking internal heat source into account. On the other hand, the physical origin of efficiency droop under self-heating effect is comprehensively analyzed and compared between the two LEDs.

2 Device structure and parameter

Two LED structures were used in this paper (named as LED A and LED B, respectively). The epitaxial wafer of LED A was prepared on a 100-μm-thick c-plane (0001) sapphire substrate. Before the growth of multiple quantum wells (MQWs) active region, a 50-nm-thick un-doped GaN buffer layer was deposited, and then a 3-μm-thick Si-doped n-type GaN layer was grown (n-doping = 5×10^{18} cm^{-3}). The active region consists of five 2.5-nm-thick $In_{0.15}Ga_{0.85}N$ quantum wells, separated by six 9-nm-thick GaN barriers. On top of the active region was a 150-nm-thick p-type GaN cap layer (p-doping = 1.2×10^{18} cm^{-3}). The structure of LED B is the same as that of LED A except for a 20-nm-thick p-type $Al_{0.38}Ga_{0.46}In_{0.16}N$ EBL (p-doping = 1.2×10^{18} cm^{-3}) that was placed between the active region and p-type GaN layer. The mesa size was designed with a rectangular shape of 300 μm × 300 μm. The schematic diagrams of the two LED structures under study are shown in Fig. 1.

The LED optical and electrical properties were numerically investigated with the APSYS simulation program developed by Crosslight Software Inc., which solves Poisson's equation, current continuity equations, carrier transport equation, quantum mechanical wave equation, and photon rate equation. The non-radiative recombination processes and current leakage are taken into account in the calculation. The software employs the 6 × 6 $k\,p$ model to calculate the energy band structures, which was developed by Chuang and Chang [44, 45]. The band gap energy of InN, GaN, and AlN as a function of temperature T can be expressed by the Varshni formula [46]:

$$E_g(T) = E_g(0) - \frac{\alpha \cdot T^2}{T + \beta}, \tag{1}$$

where $E_g(T)$ is the band gap energy at temperature T, $E_g(0)$ is the band gap energy at 0 K, and α and β are material related constants. The values of $E_g(0)$, α and β for InN, GaN, and AlN are listed in Table 1. For ternary alloys of InGaN and AlGaN, the band gap energies can be expressed as follows [46]:

$$E_g(In_xGa_{1-x}N) = E_g(InN) \cdot x + E_g(GaN) \cdot (1-x) - b(InGaN) \cdot x \cdot (1-x), \tag{2}$$

$$E_g(Al_xGa_{1-x}N) = E_g(AlN) \cdot x + E_g(GaN) \cdot (1-x) - b(AlGaN) \cdot x \cdot (1-x), \tag{3}$$

where E_g $(In_xGa_{1-x}N)$ and E_g $(Al_xGa_{1-x}N)$ are the band gap energies of $In_xGa_{1-x}N$ and $Al_xGa_{1-x}N$, the bowing parameters for InGaN and AlGaN are 1.43 and 1.0 eV, respectively. The energy band gap of $Al_xGa_{1-x-y}In_yN$ can be expressed as the following formulas:

$$E_g(Al_xGa_{1-x-y}In_yN) = \frac{xyE_g(AlInN) + yzE_g(InGaN) + zxE_g(AlGaN)}{xy + yz + zx}, \tag{4}$$

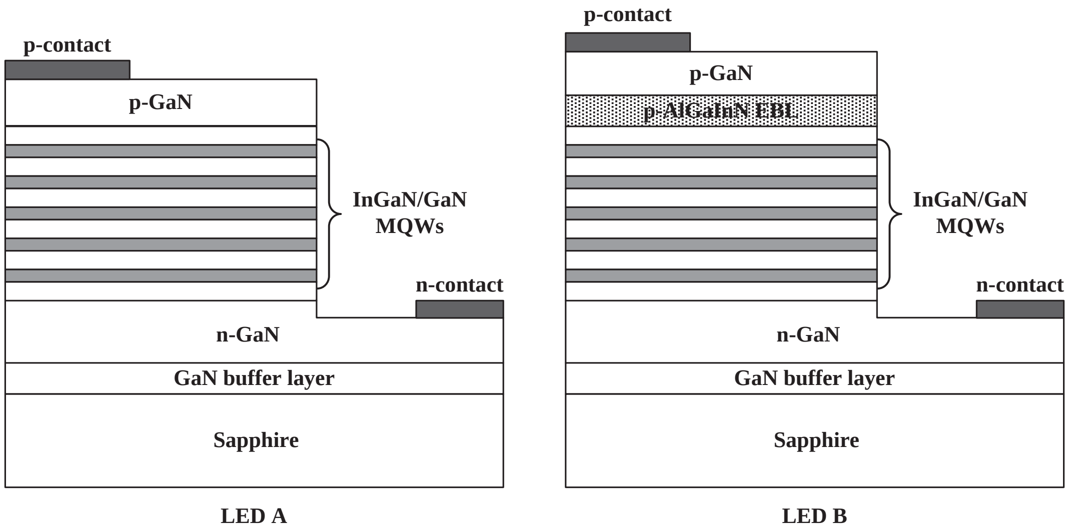

Fig. 1 Schematic diagrams for LEDs A and B

Table 1 Material parameters used in the simulation for the binary semiconductor compound

Material	E_g (0) (eV)	α (meV K^{-1})	β (K)
InN	0.735	0.245	624
GaN	3.507	0.909	830
AlN	6.230	1.799	1,462

$$E_g(\text{AlInN}) = uE_g(\text{InN}) + (1-u)E_g(\text{AlN}) - u(1-u)b(\text{AlInN}), \quad (5)$$

$$E_g(\text{InGaN}) = vE_g(\text{GaN}) + (1-v)E_g(\text{InN}) - v(1-v)b(\text{InGaN}), \quad (6)$$

$$E_g(\text{AlGaN}) = wE_g(\text{GaN}) + (1-w)E_g(\text{AlN}) - w(1-w)b(\text{AlGaN}), \quad (7)$$

$$u = \frac{1-x+y}{2}, \quad v = \frac{1-y+x}{2}, \quad w = \frac{1-x+z}{2}, \quad (8)$$

where x, y, and $z = 1 - x - y$ are the compositions of Al, In, and Ga in the AlGaInN material, respectively. The bowing parameter for $Al_xIn_{1-x}N$ is 2.5 eV. Other material parameters of the semiconductors used in the simulation can be found in [47].

The charge density induced by the spontaneous and piezoelectric polarization at the hetero interface can be calculated by the method developed by Fiorentini et al. [48]. The total polarization is the sum of the spontaneous and piezoelectric polarization. Considering the screening caused by defects, the surface charge densities are generally varied from 20 % to 80 % as compared to that of theoretical calculations [49, 50]. In this study, the interface charge density is assumed to be 50 % of the calculated values [35].

The Caughey–Thomas approximation [51] is employed in the simulation for the carrier mobility as a function of carrier density which can be expressed as follows:

$$\mu_i(N) = \mu_{\min,i} + \frac{\mu_{\max,i} - \mu_{\min,i}}{1.0 + \left(\frac{N}{N_{\text{ref},i}}\right)^{\alpha,i}}, \quad (9)$$

where i denotes either electron or hole, the values of all parameters in the formula are listed in Table 2.

The total recombination rate in the LED device consists of non-radiative recombination rate, radiative recombination rate, and Auger recombination rate, which can be expressed as the rate equation model [34]:

$$R_{\text{total}} = An + Bn^2 + Cn^3, \quad (10)$$

where A, B, C, and n are the non-radiative coefficient, radiative coefficient, Auger coefficient, and carrier density, respectively. The total injection current consists of radiative recombination current that generates photons in the quantum wells (I_{rad}) and lost current. Generally, the lost current occurs either inside or outside of the quantum wells. The lost current inside of the quantum wells (non-radiative recombination processes) consists of Shockley–Read–Hall (SRH) recombination current (I_{SRH}) and Auger recombination current (I_{Auger}). The lost current outside of the quantum wells is current leakage (I_{leak}). As a result, the total injection current can be written as follows:

$$I = I_{\text{rad}} + I_{\text{SRH}} + I_{\text{Auger}} + I_{\text{leak}}. \quad (11)$$

The internal quantum efficiency can be defined as the radiative recombination current inside the quantum wells divided by the total injection current I which can be expressed as:

Table 2 Material parameters used in the simulation for carrier mobility

Material	$\mu_{max,n}$ ($cm^2 V^{-1} s^{-1}$)	$\mu_{min,n}$ ($cm^2 V^{-1} s^{-1}$)	$N_{ref,n}$ (cm^{-3})	α_n	$\mu_{max,p}$ ($cm^2 V^{-1} s^{-1}$)	$\mu_{min,p}$ ($cm^2 V^{-1} s^{-1}$)	$N_{ref,p}$ (cm^{-3})	α_p
AlGaN	306	132	1×10^{17}	0.29	10	10	3×10^{17}	0.395
InGaN	684	386	1×10^{17}	1.37	2	2	2.75×10^{17}	0.395

$$\eta_{IQE} = \frac{I_{rad}}{I} = \frac{I_{rad}}{I_{rad} + I_{SRH} + I_{Auger} + I_{leak}}. \quad (12)$$

According to heat generation mechanism in semiconductor materials, the internal heat source consists of Joule heat, carrier recombination heat, Thomson heat, and Peltier heat [52]. It has been reported that the Joule heat and recombination heat contribute the major part of the whole heat generation. The Thomson heat and Peltier heat contribute less so that they can be neglected [53]. Thus, only the Joule heat and recombination heat were taken into account in this study. When carrier moves from a higher electrostatic potential to a lower potential in the device, the corresponding energy difference is absorbed by the lattice as Joule heat; it can be expressed as [52]

$$H_J = -\frac{1}{q}\left(\vec{j}_n \nabla E_{Fn} + \vec{j}_p \nabla E_{Fp}\right), \quad (13)$$

where q is the electronic charge; $\vec{j}_n$ and $\vec{j}_p$ are electron and hole current density, respectively; and E_{Fn} and E_{Fp} are electron and hole quasi-Fermi level, respectively. When an electron–hole pair recombines, the energy either converts to light (photon) or heat (phonon). For each electron–hole pair recombination, the released heat is the difference between the electron and hole quasi-Fermi levels [52]:

$$H_R = R(E_{Fn} - E_{Fp}), \quad (14)$$

where, the recombination rate $R = R_{SRH} + R_{Aug}$, R_{SRH} and R_{Aug} are the Shockly–Read–Hall recombination rate and Auger recombination rate, respectively. The thermal conductivities for each layer of the LED device are list in Table 3 [54]. It should be noted that the thermal conductivity in MQWs is quite different from that of bulk materials due to phonon confinement effects and interface effects [54]. Hence, the anisotropic thermal conductivity was used in MQWs, and the thermal conductivities of k_L for the lateral direction and k_V for the vertical direction are smaller than those of the bulk materials [54]. The LEDs were loaded onto the copper submount. We assume that the submount temperature was controlled with a thermoelectric cooler and a thermistor at a constant temperature 300 K in the oven. To simply the simulation, we treated the other faces of the LED adiabatic [55].

In the simulation, Auger recombination coefficient will be varied in order to investigate its effect on the internal quantum efficiency under self-heating effect. Other simulation parameters of the LEDs used in the simulation are taken from Ref. [21], in which the advantage of blue GaN-based LEDs with InGaN barriers are investigated, their simulation results are in good agreement with experimental data. The model validation has been performed in our previous paper [56], more details can be found in [56].

Table 3 Material thermal conductivities used in the simulation

Name	Material	Thermal conductivity ($W\ mK^{-1}$)	Thickness (μm)
Sapphire substrate	Al_2O_3	38	100
n-Buffer layer	GaN	177	0.05
n-Type GaN layer	GaN	177	3
Active region	InGaN(well)/ GaN(barrier)	$k_L = 134.3$, $k_V = 22.8$	0.0665
EBL	AlGaInN	69	0.02
p-Type GaN layer	GaN	177	0.15

3 Results and discussion

The energy band profile strongly influences the carrier transport characteristic. Figure 2 shows the energy band diagrams and quasi-Fermi levels near the EBL and p-type GaN barrier of LEDs A and B at 120 mA. The effective barrier height for carriers is defined as the energy difference between the maximum energy of the EBL (or p-type layer) and the quasi-Fermi level in front of the EBL. As indicated in Fig. 2, the effective barrier height for confining electron in the conduction band is only 238 meV for LED A without an EBL. However, when the AlGaInN EBL is employed, the effective barrier height is increased from 238 to 386 meV. It is apparent that the effective barrier height for preventing electron overflow in LED B is substantially enhanced. Moreover, in the valence band of LED B, the obstacle effective barrier height for holes is reduced from 267 to 222 meV, which improves the efficiency of hole injection into the MQWs. Consequently, when a p-type AlGaInN layer was inserted between the p-type

GaN layer and the active region, the relatively larger band gap energy and better lattice-match of AlGaInN layer can not only increase the effective barrier height in the conduction band but also decrease the obstacle effective barrier height for hole injection in the valence band. According to this proper modified energy band diagram, the diminished electron overflow and enhanced hole injection efficiency can be expected. This could be justified by the vertical electron current leakage profiles of the two LEDs (see Fig. 3).

Figure 3 shows the electron current density near the active region at injection current of 120 mA. The electrons are injected from n-type GaN layer into the MQWs and then recombine with holes, which results in the decrease of electron current density along the growth direction. The electron current overflowing from the MQWs to the p-type layer is viewed as current leakage. As shown in Fig. 3, it is evident that the electron leakage overflowing to the p-type GaN layer of LED A is quite serious which indicates insufficient electron blocking. When the AlGaInN EBL is employed, the electron leakage is substantially reduced due to the better electron confinement ability. The value is almost decreased to zero. Therefore, more electrons will stay in the active region to recombine with holes. This is consistent with the improved modified energy band diagrams in Fig. 2.

When the electrons overflowing to the p-type layer are diminished, the electron concentration in the active region should be increased. Moreover, hole injection efficiency into the active region could be also enhanced because there are fewer holes that would recombine with leaked electrons before they are injected into the active region. This can be further justified by comparison of the electron and hole concentrations in the MQWs as shown in Fig. 4. In all of the quantum wells, both electron and hole concentrations of LED B increase. The concentrations of electrons and holes within the active region are enhanced by 72.2 % and 73.5 % for LED B, respectively, when compared to LED A. Figure 5a shows the radiative recombination rates for LEDs A and B in the active region at 120 mA, respectively. It is evident that, due to the reduced electron current leakage and increased hole injection efficiency, the radiative recombination rates are enhanced in every quantum well for LED B. Consequently, the efficiency droop for LED B is significantly improved. Figure 6 shows the IQE and light output power curves for LEDs A and B as a function of injection current. The efficiency droops, which are defined as the formula $(IQE_{peak} - IQE_{min})/IQE_{peak}$, are 57 % and 0 % for LEDs A and B, respectively. The enhanced IQE leads to the improved output power. As the AlGaInN EBL was used, the output power is improved by a factor of 1.92 at 120 mA, and the efficiency droop does not occur.

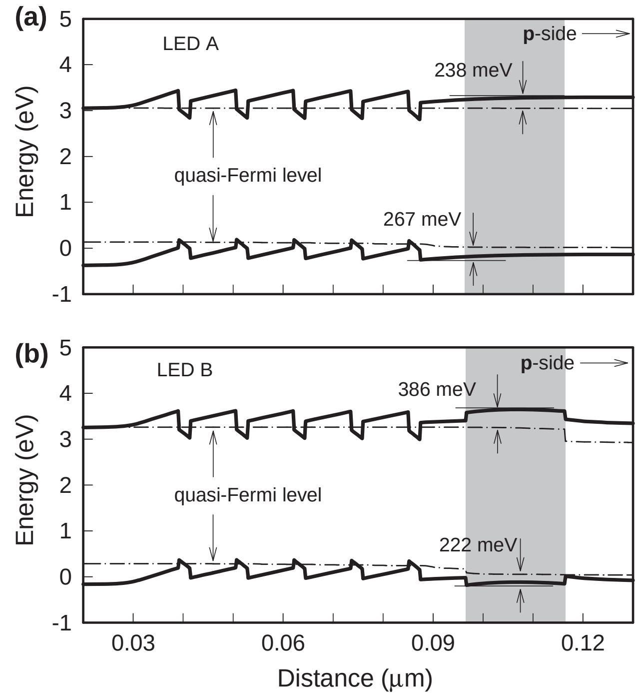

Fig. 2 Energy band diagrams for **a** LED A and **b** LED B at 120 mA

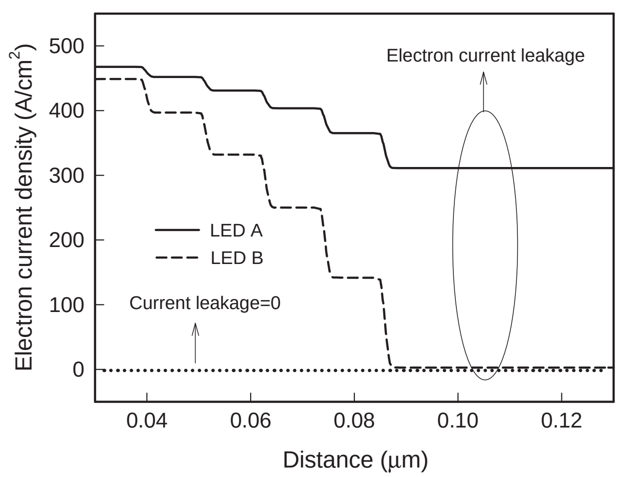

Fig. 3 Electron current density near the active region for **a** LED A and **b** LED B at 120 mA

The internal heat characteristic is strongly influenced by the carrier transport mechanism. As indicated in Fig. 7, for LED A, the contribution difference between Joule heat and recombination are small, Joule heat is a little higher than recombination heat due to the serious electron current leakage. For LED B, recombination heat contributes the major part of the heat generation. This result is consistent with the carrier recombination and electron current leakage profiles. Figure 5b, c shows that non-radiative recombination rate of LED B is higher than that of LED A at 120 mA,

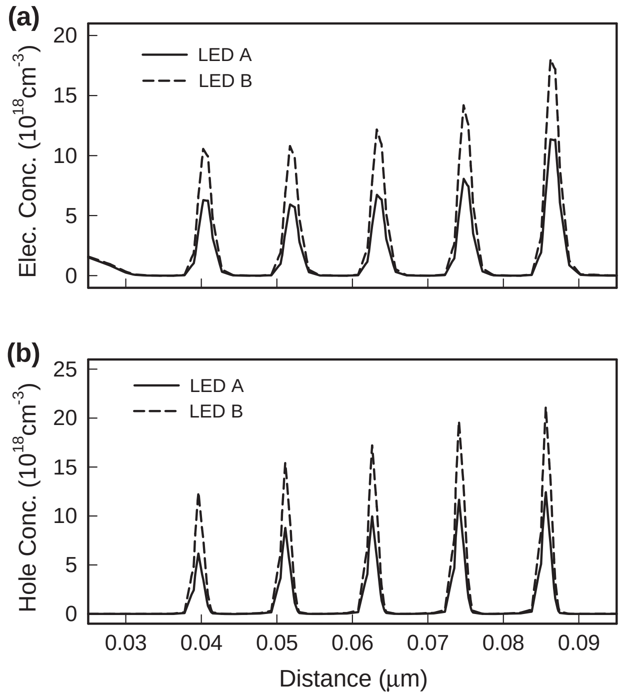

Fig. 4 **a** Electron concentration and **b** hole concentration within the MQWs for LEDs A and B at 120 mA

which leads to the raised non-radiative recombination heat (see Eq. 14). The difference of non-radiative recombination heat between the two LEDs becomes obvious at larger injection current. However, the Joule heat is reduced for LED B due to decreased electron leakage by introducing an EBL. It is also indicated from Fig. 7 that, with the injection current increased, the enhance degree of recombination heat is larger than the reduced degree of Joule heat for LED B. Thus, the combination effect of Joule heat and recombination heat causes the enhanced total heat source intensity, the total heat increases faster than that of LED A after introducing the AlGaInN EBL structure.

The heat power difference and maximum chip temperature as a function of injection current for both LEDs are shown in Fig. 8. It indicates that the maximum chip temperature for both LEDs increases with increasing injection current. Because heat power difference between the two LEDs becomes larger with the increased injection current, the maximum chip temperature of LED B with AlGaInN EBL increases faster than that of LED A without EBL. When the current increases to 120 mA, the chip temperature of LED B is 335 K, which is much higher than 321 K of LED A without EBL. Though LED B holds a higher chip temperature than LED A across the whole injection current range, it shows no efficiency droop. On the contrary, LED A holds a lower chip temperature, but it shows serious efficiency droop (see Fig. 6). This illustrates that

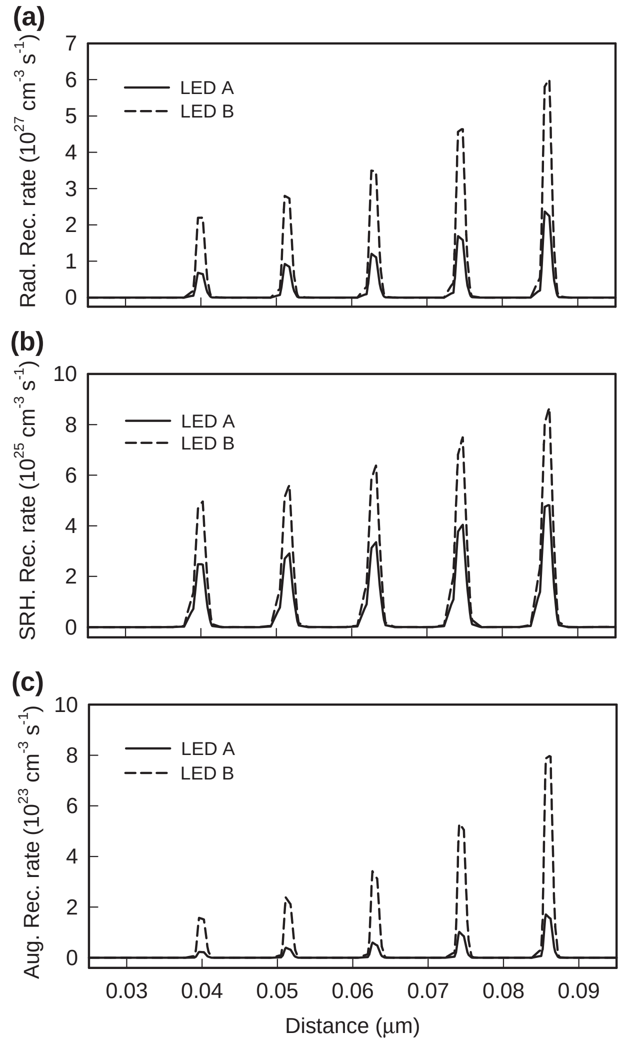

Fig. 5 **a** Radiative recombination rate, **b** SRH recombination rate, and **c** Auger recombination rate within the MQWs for LEDs A and B at 120 mA

self-heating effect may not be the mechanism responsible for efficiency droop.

Most publications only discussed one possible mechanism of efficiency droop, such as those listed in the introduction. In this segment, we demonstrate that the efficiency droop is caused by multiple factors. Auger recombination coefficients of GaN materials are reported within the range from 1×10^{-34} to 1×10^{-30} $cm^6\ s^{-1}$ based on different theoretical and experiment estimations [38, 39]. Based on isothermal model, it has been reported that Auger recombination in GaN-based MQWs LEDs is one of the debate issues on efficiency droop. In order to clarify the effect of Auger recombination on the efficiency droop under self-heating effect, the internal quantum efficiency as a function of injection current was calculated for both small and large Auger coefficients.

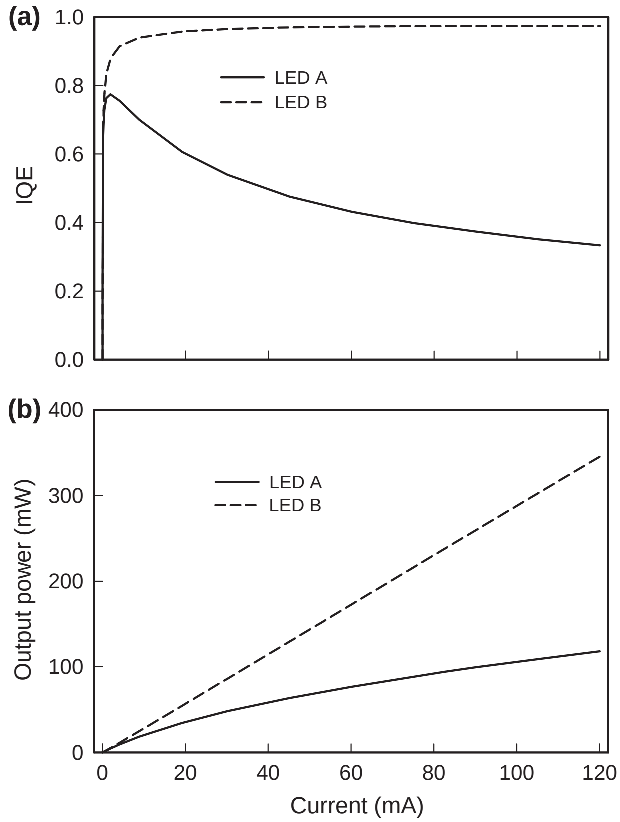

Fig. 6 **a** Internal quantum efficiency and **b** output power as a function of injection current for LEDs A and B

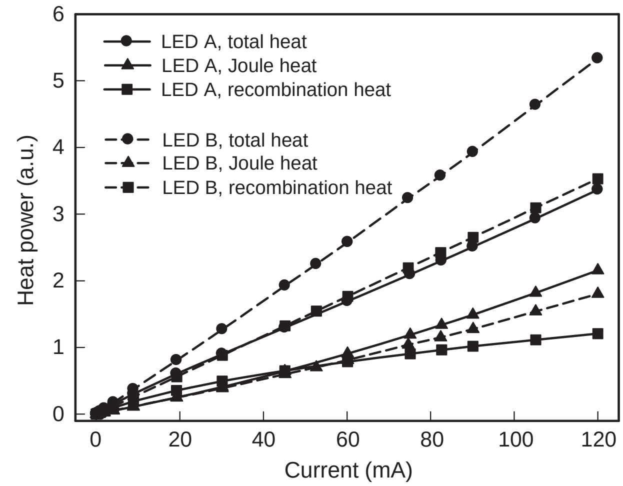

Fig. 7 Internal heat source (Joule heat, non-radiative recombination heat, and total heat, respectively) characteristics as a function of injection current for LEDs A and B

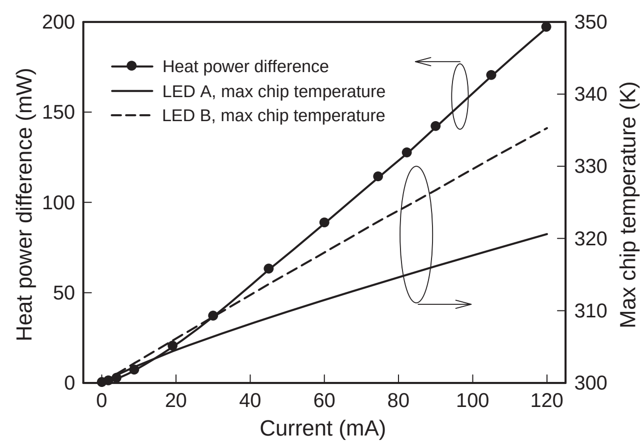

Fig. 8 Heat power difference and maximum chip temperature as a function of injection current for LEDs A and B

With self-heating, effect of different Auger coefficients on internal quantum efficiency of LEDs A and B are shown in Fig. 9a, b, respectively. For LED A, there exists efficiency droop for both small and large Auger coefficients, and the efficiency droop becomes serious with a larger Auger recombination rate (droop ratio is increased from 57 % to 66 %). For LED B, there is no efficiency droop for a small Auger coefficient ($C = 1 \times 10^{-34}$ cm^6 s^{-1}), however, when Auger coefficient is increased to 1×10^{-30} cm^6 s^{-1}, 30 % efficiency droop ratio is observed. Consequently, Auger recombination may be another mechanism of efficiency droop under self-heating effect besides electron current leakage.

To further compare the self-heating effect on efficiency droop under different Auger coefficients, the max chip temperatures for LED A and LED B as a function of injection current with small and large Auger coefficients are plotted in Fig. 10 (LED A) and Fig. 11 (LED B). It is indicated that, for LED A, the heat power difference between small and larger Auger coefficient is only 2 mW at injection current of 120 mA. As for LED B, the heat power difference between small and larger Auger coefficient is larger than LED A, but it is also very small compared to the total heat power, only 7 mW at injection current of 120 mA. Consequently, non-radiative Auger recombination heat is not the major contributor for internal heat source and it can be neglected. Increasing Auger recombination rate caused little chip temperature change. Based on above results, keeping the almost same chip temperature, efficiency droop of LED A becomes more serious with increased Auger recombination rate. For LED B, small Auger recombination rate shows no efficiency droop, but larger rate shows serious efficiency droop. It indicates again that self-heating is not the mechanism responsible for efficiency droop. From the experiment data reported by Kim et al. [11], the magnitude of droop decreases with increasing temperature, therefore, temperature does not caused efficiency droop. This is consistent with our simulation results.

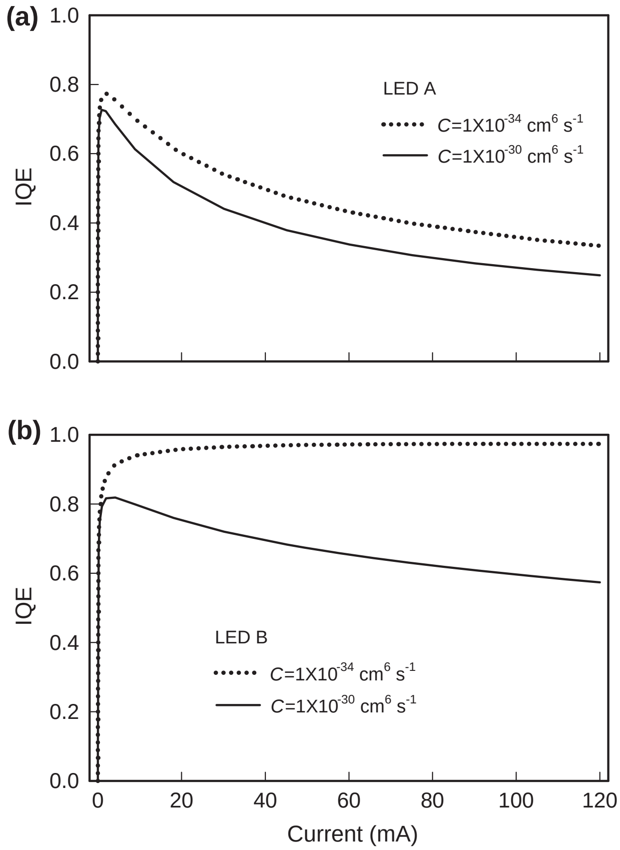

Fig. 9 Internal quantum efficiencies as a function of injection current for **a** LED A and **b** LED B with various Auger recombination coefficients

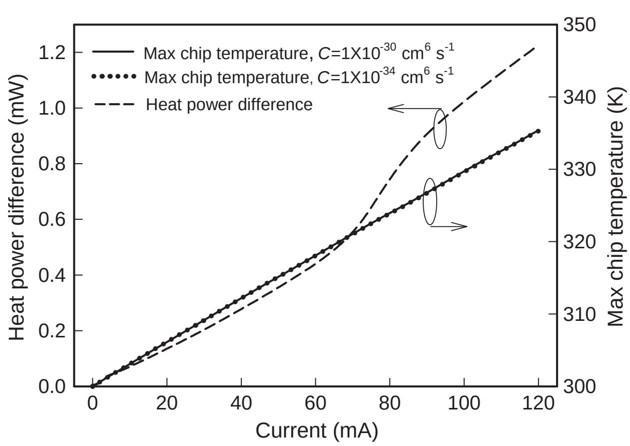

Fig. 10 Heat power difference and maximum chip temperature as a function of injection current for LED A with various Auger recombination coefficients

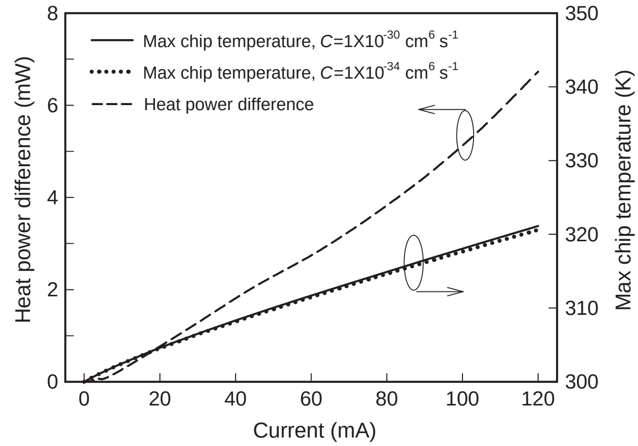

Fig. 11 Heat power difference and maximum chip temperature as a function of injection current for LED B with various Auger recombination coefficients

4 Conclusion

In this paper, two LEDs without EBL (LED A) and with AlGaInN EBL (LED B) are used to investigate the effect of EBL on the characteristic of GaN-based light-emitting diodes under self-heating effect. In the simulation, internal Joule heat and recombination heat are taken into account. The origin of efficiency droop mechanism under self-heating effect is also analyzed. The results are as follows:

(1) Compared with LED A, AlGaInN EBL in LED B can not only increase the electron effective barrier height in the conduction band but also decrease the hole obstacle barrier height in the valence band. Thus, the electron current leakage is markedly reduced, and the hole injection efficiency is significantly enhanced. This leads to improved efficiency droop characteristic. Electron current leakage is one of the responsible mechanisms for efficiency droop.

(2) Compared with LED A, non-radiative recombination heat is enhanced but Joule heat is decreased when AlGaInN EBL is introduced in LED B. However, the enhance degree of recombination heat is larger than the reduced degree of Joule heat. Hence, it causes enhanced total internal heat source intensity and higher chip temperature than LED A. The chip temperature of LED B is 335 K at 120 mA, which is higher than LED A with 321 K.

(3) With small Auger recombination rate, though LED B holds higher chip temperature than LED A across the whole injection current range, it shows no efficiency droop. On the contrary, LED A holds lower chip temperature, but it shows serious efficiency droop. This illustrates that self-heating effect may not be the mechanism responsible for efficiency droop.

(4) Auger recombination heat is not the major contributor for internal heat source and it can be neglected. Increasing Auger recombination rate caused little chip temperature change. Auger recombination is one of the responsible mechanisms for efficiency droop.

Acknowledgments This work was supported by the National Natural Science Foundation of China (U1034004, 51210011, 50825603) and the Fundamental Research Funds for the Central Universities, China (12QX14).

References

1. Schubert EF, Kim JK (2005) Solid-state light sources getting smart. Science 208:1274–1278
2. Krames MR, Shchekin OB, Mueller-Mach R et al (2007) Status and future of high-power light-emitting diodes for solid-state lighting. J Disp Technol 3:160–175
3. Crawford MH (2009) LEDs for solid-state lighting: performance challenges and recent advances. IEEE J Sel Top Quantum Electron 15:1028–1040
4. Niu QL, Zhang Y, Wang YL et al (2012) High-efficiency conjugated-polymer-hosted blue phosphorescent light-emitting diodes. Chin Sci Bull 57:3639–3643
5. Xu YQ, Fan GH, Zhou DT et al (2012) Advantage of dual wavelength light-emitting diodes with dip-shaped quantum wells. Chin Sci Bull 57:2562–2566
6. Zhang WW, Wu ZX, Zhang XW et al (2011) Dependence of the stability of organic light-emitting diodes on driving mode. Chin Sci Bull 56:2210–2214
7. Jiang HJ (2011) Effective adjustment of the optoelectronic properties of organic conjugated materials by synthesizing p–n diblock molecules. Chin Sci Bull 56:119–136
8. Meng LC, Lou ZD, Yang SY et al (2011) Energy distribution in white organic light-emitting diodes with three primary color emitting layers. Sci China Phys Mech Astron 54:84–88
9. Wang XL, Wang XH, Jia HQ et al (2010) Recent progress in single chip white light-emitting diodes with the InGaN underlying layer. Sci China Phys Mech Astron 53:445–448
10. Zhen H, Xiong D, Zhou X et al (2006) Study on the p-type QWIP-LED device. Sci China G Phys Mech Astron 49:401–410
11. Kim MH, Schubert MF, Dai Q et al (2007) Origin of efficiency droop in GaN-based light-emitting diodes. Appl Phys Lett 91:183507
12. Schubert MF, Xu J, Kim JK et al (2008) Polarization-matched GaInN/AlGaInN multi-quantum-well light emitting diodes with reduced efficiency droop. Appl Phys Lett 93:041102
13. Choi S, Kim HJ, Kim SS et al (2010) Improvement of peak quantum efficiency and efficiency droop in III-nitride visible light-emitting diodes with an InAlN electron-blocking layer. Appl Phys Lett 96:221105
14. Wang CH, Chen JR, Chiu CH et al (2010) Temperature dependent electroluminescence efficiency in blue InGaN–GaN light emitting diodes with different well widths. IEEE Photon Technol Lett 22:236–238
15. Zhao HP, Liu GY, Zhang J et al (2011) Approaches for high internal quantum efficiency green InGaN light-emitting diodes with large overlap quantum wells. Opt Express 19:A991–A1007
16. Ding K, Zeng YP, Wei XC et al (2009) A wide-narrow well design for understanding the efficiency droop in InGaN/GaN light-emitting diodes. Appl Phys B 97:465–468
17. Li YL, Huang YR, Lai YH (2007) Efficiency droop behaviors of InGaN/GaN multiple-quantum-well light-emitting diodes with varying quantum well thickness. Appl Phys Lett 91:181113
18. Han SH, Lee DY, Shim HW et al (2010) Improvement of efficiency droop in InGaN/GaN multiple quantum well light-emitting diodes with trapezoidal wells. J Phys D 43:354004
19. Lee YJ, Chen CH, Lee CJ (2010) Reduction in the efficiency-droop effect of InGaN green light-emitting diodes using gradual quantum wells. IEEE Photon Technol Lett 22:1506–1508
20. Chang JY, Tsai MC, Kuo YK (2010) Advantages of blue InGaN light-emitting diodes with AlGaN barriers. Opt Lett 35:1368–1370
21. Kuo YK, Chang JY, Tsai MC et al (2009) Advantages of blue InGaN multiple-quantum well light-emitting diodes with InGaN barriers. Appl Phys Lett 95:011116
22. Kuo YK, Wang TH, Chang JY (2012) Advantages of blue InGaN light-emitting diodes with InGaN–AlGaN–InGaN barriers. Appl Phys Lett 100:031112
23. Liu JP, Ryou JH, Dupuis RD et al (2008) Barrier effect on hole transport and carrier distribution in InGaN/GaN multiple quantum well visible light-emitting diodes. Appl Phys Lett 93:021102
24. Tsai MC, Yen SH, Kuo YK (2011) Deep-ultraviolet light-emitting diodes with gradually increased barrier thicknesses from n-layers to p-layers. Appl Phys Lett 98:111114
25. Wang CH, Chang SP, Ku PH et al (2011) Hole transport improvement in InGaN/GaN light-emitting diodes by graded-composition multiple quantum barriers. Appl Phys Lett 99:171106
26. Ni X, Fan Q, Shimada R et al (2008) Reduction of efficiency droop in InGaN light emitting diodes by coupled quantum wells. Appl Phys Lett 93:171113
27. Han SH, Lee DY, Lee SJ et al (2009) Effect of electron blocking layer on efficiency droop in InGaN/GaN multiple quantum well light-emitting diodes. Appl Phys Lett 94:231123
28. Yen SH, Tsai MC, Tsai ML et al (2009) Effect of n-type AlGaN layer on carrier transportation and efficiency droop of blue InGaN light-emitting diodes. IEEE Photon Technol Lett 21:975–977
29. Lee KB, Parbrook PJ, Wang T et al (2009) Effect of the AlGaN electron blocking layer thickness on the performance of AlGaN-based ultraviolet light-emitting diodes. J Cryst Growth 311:2857–2859
30. Xia CS, Li ZM, Lu W et al (2012) Efficiency enhancement of blue InGaN/GaN light-emitting diodes with an AlGaN–GaN–AlGaN electron blocking layer. J Appl Phys 111:094503
31. Kuo YK, Chang JY, Tsai MC (2010) Enhancement in hole-injection efficiency of blue InGaN light-emitting diodes from reduced polarization by some specific designs for the electron blocking layer. Opt Lett 35:3285–3287
32. Wang CH, Ke CC, Lee CY et al (2010) Hole injection and efficiency droop improvement in InGaN/GaN light-emitting diodes by band-engineered electron blocking layer. Appl Phys Lett 97:261103
33. Xia CS, Li ZM, Lu W et al (2011) Droop improvement in blue InGaN/GaN multiple quantum well light-emitting diodes with indium graded last barrier. Appl Phys Lett 99:233501
34. Kuo YK, Tsai MC, Yen SH et al (2010) Effect of p-type last barrier on efficiency droop of blue InGaN light-emitting diodes. IEEE J Quantum Electron 46:1214–1220
35. Kuo YK, Shih YH, Tsai MC et al (2011) Improvement in electron overflow of near-ultraviolet InGaN LEDs by specific design on last barrier. IEEE Photon Technol Lett 23:1630–1632
36. Yen SH, Tsai ML, Tsai MC et al (2010) Investigation of optical performance of InGaN MQW LED with thin last barrier. IEEE Photon Technol Lett 22:1787–1789
37. Chen JR, Lu TC, Kuo HC et al (2010) Study of InGaN–GaN light-emitting diodes with different last barrier thicknesses. IEEE Photon Technol Lett 22:860–862
38. Shen YC, Mueller GO, Watanabe S et al (2007) Auger recombination in InGaN measured by photoluminescence. Appl Phys Lett 91:141101
39. Chen JR, Wu YC, Ling SC et al (2010) Investigation of wavelength-dependent efficiency droop in InGaN light-emitting diodes. Appl Phys B 98:779–789
40. Efremov AA, Bochkareva NI, Gorbunov RI et al (2006) Effect of the Joule heating on the quantum efficiency and choice of thermal

conditions for high-power blue InGaN/GaN LEDs. Semiconductors 40:605–610
41. Chen YX, Shen GD, Guo WL et al (2011) Internal quantum efficiency drop induced by the heat generation inside of light emitting diodes (LEDs). Chin Phys B 20:017204
42. Hirayama H (2005) Quaternary InAlGaN-based high-efficiency ultraviolet light-emitting diodes. J Appl Phys 97:091101
43. Ryu HY, Shim JI, Kim CH et al (2011) Efficiency and electron leakage characteristics in GaN-based light-emitting diodes without AlGaN electron-blocking-layer structures. IEEE Photon Technol Lett 23:1866–1868
44. Chuang SL, Chang CS (1996) *k·p* method for strained wurtzite semiconductors. Phys Rev B 54:2491–2504
45. Chuang SL, Chang CS (1997) A band-structure model of strained quantum-well wurtzite semiconductors. Semicond Sci Technol 12:252–263
46. Vurgaftman I, Meyer JR, Ram-Mohan LR (2001) Band parameters for III–V compound semiconductors and their alloys. J Appl Phys 89:5815–5875
47. Vurgaftman I, Meyer JR (2003) Band parameters for nitrogen containing semiconductors. J Appl Phys 94:3675–3696
48. Fiorentini V, Bernardini F, Ambacher O (2002) Evidence for nonlinear macroscopic polarization in III–V nitride alloy heterostructures. Appl Phys Lett 80:1204–1206
49. Renner F, Kiesel P, Döhler GH et al (2002) Quantitative analysis of the polarization fields and absorption changes in InGaN/GaN quantum wells with electroabsorption spectroscopy. Appl Phys Lett 81:490–492
50. Zhang H, Miller EJ, Yu ET et al (2004) Measurement of polarization charge and conduction-band offset at $In_xGa_{1-x}N$/GaN heterojunction interfaces. Appl Phys Lett 84:4644–4646
51. Caughey CM, Thomas RE (1967) Carrier mobilities in silicon empirically related to doping and field. Proc IEEE 55:2192–2193
52. Piprek J (2003) Semiconductor optoelectronic devices: introduction to physics and simulation. Academic press, San Diego, pp 145–147
53. Wang TH, Xu JL, Wang XD (2012) The effect of multi-quantum barrier structure on light-emitting diodes performance by a non-isothermal model. Chin Sci Bull 57:3937–3942
54. Lee HK, Yu JS, Lee YT (2010) Thermal analysis and characterization of the effect of substrate thinning on the performances of GaN-based light emitting diodes. Phys Status Solidi A 207:1497–1504
55. Huang S, Wu H, Fan B et al (2010) A chip-level electro thermal coupled design model for high-power light-emitting diodes. J Appl Phys 107:054509
56. Xu JL, Wang TH (2013) Efficiency droop improvement for InGaN-based light-emitting diodes with gradually increased in-composition across the active region. Phys E 52:8–13